UNEC Journal of Engineering and Applied Sciences
Vol. 4, No.2, 2024, pp. 20-36
DOI: https://doi.org/10.61640/ujeas.2024.1203

SECTION: CHEMISTRY & MATERIALS SCIENCE

Synthesis, characterization and measurement of antimicrobial activity of (6Z,15Z)-4,18-dioxa-9,13-dithia-7,15-diaza-1,2(1,4),5,8,11,14,17(1,2)-heptabenzenecyclononadecaphan-6,15-diliene and its palladium(II) chloride complex

M. Türkyılmaz*, M. Dönmez, N.B. Gür

Department of Chemistry, Faculty of Sciences, Trakya University Balkan Campus, Edirne 22030, Türkiye
email: mturkyilmaz@trakya.edu.tr

Abstract

To synthesize the Schiff base with the desired properties, a transition from a monomeric molecule to a macrocyclic structure was made. For this purpose; (oxy)-dibenzaldehyde dibenzaldehyde derivative, (oxy)bis(*N*-prop)-1-en-2-yl-aniline derivative, (oxy)-dianiline derivative and (sulfanediyl)-dianiline compounds were obtained at the end of four different reaction processes. In the last step of these reactions, a macrocyclic compound (6Z,15Z)-4,18-dioxa-9,13-dithia-7,15-diaza-1,2(1,4),5,8,11,14,17(1,2)-heptabenzenecyclononadecaphan-6,15-diene Schiff base was obtained by condensation method. As a result of the reaction of this product with $PdCl_2$, (6Z,15Z)-4,18-dioxa-9,13-dithia-7,15-diaza-1,2(1,4),5,8,11,14,17(1,2)-heptabenzenecyclononadecaphan-6,15-dylene palladium(II) chloride product was obtained and a new biologically active metal complex was synthesized. Their structures were identified by characterizing them according to elemental analysis (C, H, N), thermal analysis, PXRD, conductivity measurements, FT-IR, and UV-vis spectra. Spectral data confirmed the structure of azomethine (-C=N-) and phenolic OH groups with a nitrogen atom of the metal-coordinated ligand and the presence of metal ions. As a result of this information, a tetrahedral geometry was suggested for the Pd(II) complex. Antimicrobial activities of the synthesized metal complex were tested. Pd(II) complex showed the highest cytotoxicity (MIC value 11.25±0.14 µg/mL) effect, comparable to other cis-platinum-based drugs.

***Keywords*:** Schiff base, paladium, antimicrobial measurement, TGA analysis, conductivity.

PACS numbers: 74.25.Fy, 76.30.Da, 83.85.Fg

Received:	*Revised:*	*Accepted:*	*Published:*
7 October 2024	*22 October 2024*	*25 October 2024*	*26 December 2024*

1. Introduction

1.1. Background on Schiff Bases

Because of their significance and biological activity contrary to bacteria, fungi, malignant tumors, and other organisms, mixed chelated mineral complexes have recently drawn attention [1]. Schiff bases, which were first synthesized in 1964 and named after Hugo Schiff [2], are a general compound in organic chemistry with the general structure $R_1R_2C=NR_3$ (R_3 = alkyl or aryl, but not hydrogen). Pfeiffer was the first to use Schiff bases as ligands, which were considered to be a very important opportunity for coordination

compounds [3]. This is because small-molecule compounds such as cyano (C≡N), amine (-NH_2), and oxalate (-$C_2O_4^{2-}$) were used as ligands. Depending on their structure, they can be classified as secondary ketimines or secondary aldimines, making them a subclass of imines.

A commonly used subset of Schiff bases, known as imines derived from anilines, are called anyl. The term azomethine, which specifically refers to secondary aldimines (R−CH=NR′, where R′ ≠ H), can be used interchangeably.

Aldehydes react with primary amines to form *N*-substituted imines, which are unstable. However, resonance stabilizes Schiff bases and imines made from aromatic aldehydes, especially when there are one or two aryl groups with double bonds on the carbon atom [4]. If the preconditions for the formation of the Schiff base are not met, they can hydrolyze back to the starting materials [5]. During the formation of the coordination compound, these ligands can donate one or more electron pairs to the metal ion. Very stable 4, 5, or 6-ring complexes can be formed by Schiff bases, but this requires the presence of a secondary functional group (Hydroxyl) attached to a replaceable hydrogen atom as close as possible to the amine group [6]. These compounds have the same structural feature as the azomethine (aniles, imines) group (-HC=N-) [7,8].

1.1 Applications of Schiff bases

In an investigation, Shi et al. synthesized several Schiff bases from 5-chloro-salicylaldehyde and investigated their antimicrobial capabilities [9,10]. It has been noted that the hydrophilic or aromatic groups in the structure typically lead to an increase in the antimicrobial activities of Schiff base derivatives [11].

In general, the antimicrobial and antitumor properties of antibiotics are enhanced by metal ions. Since the majority of transition elements are found as essential elements in living organisms, they can be viewed as frameworks for metal-containing molecules in biological systems. These models can be used to explain the biological effects of metal ions and their purposes in metal-protein structures. Antibacterial [12], analgesic, antifungal [13], anticancer [14], anti-inflammatory [15], anti-HIV [16], antimalarial [17], and ulcerogenic [18] biochemical activities of Schiff bases and metal complexes have been evaluated in different qualitative and quantitative determinations. Their widespread use is quite wide in the enrichment of radioactive [19] substances [20], pharmaceuticals [21], paint industry, plastic industry [22], biology [23], agriculture [24], textile and medicine [25,26]. Ideally, it is obtained by combining the required metal ion with the previously obtained macrocyclic ligand to form a macrocyclic complex. However, due to the occurrence of undesirable polymerizations or the dominance of other by-products, the desired product can be produced in low yields during the simple synthesis of the macrocyclic compound [27,28].

1.3 Synthesis of metal bound macrocyclic complexes

When forming a coordination compound, such compounds can donate one or more electron pairs to the metal ion via the donor atom. Very stable 4, 5, or 6-ring complexes can be formed by Schiff bases, but this requires the presence of a secondary functional group (Hydroxyl) attached to a displaceable hydrogen atom as close as possible to the amine group [29]. Aldehydes react with primary amines to form *N*-substituted imines, which are unstable. However, resonance stabilizes Schiff bases and imines made from aromatic aldehydes, especially when there are one or two aryl groups with double bonds on the carbon atom. If the preconditions for the formation of the Schiff base are not met, it can hydrolyze back to the starting materials.

These compounds have the same structural characteristic, the azomethine (aniles, imines) group (-HC=N-). This active group transports a possible metal ion binding site via the nitrogen atom's hybridized orbital sp^2'lone unbonded electron pair. In azomethine derivatives, the (C=N) linkage is necessary for biological activity; many azomethines have been shown to have strong antifungal, antibacterial, anticancer, and antimalarial effects [30,31]. Formation of

imine groups between sterically oriented appropriate dicarbonyl molecules and primary diamines in the absence of metal ions in the reaction is an effective technique for Schiff base synthesis of macrocyclic complexes. In this case, the metal acts as a template and helps the active ends of the ligands to align with each other to produce [1+1] or [2+2] macrocyclic products and form complexes [32]. Here, several factors determine whether intramolecular condensation will form [1+1] or [2+2] macrocyclic complexes [33,34].

This study aims to synthesize novel Schiff base macrocyclic ligands and evaluate their antibacterial and antifungal properties and the properties of palladium complexes. The chemical structures of the synthesized compounds were characterized using FTIR, ^{1}H-NMR, ^{13}C-NMR, DEPT-NMR, LC-QTOF mass spectroscopy, elemental analysis, ICP analysis, conductivity analysis, and thermogravimetric analysis (TGA-DTA) methods [35,36]. Additionally, the antibacterial and antifungal properties of the ligands and Pd^{2+} complexes were investigated using the disk diffusion method [37,38].

2. Materials and methods

2.1. Materials

Sigma-Aldrich provided the chemicals 2-hydroxybenzaldehyde ($C_7H_6O_2$, 99%) (**1**), 4,4'-bis(chloromethyl)-1,1'-biphenyl ($C_{14}H_{12}C_2$, 99%) (**2**), *N*-(2-hydroxyphenyl)acetamide (**4**) ($C_8H_9NO_2$, 99%), 2-aminobenzenethiol (**8**) (C_6H_7NS, 99%) and 1,2-bis(bromomethyl)benzene (**9**) (C_8H_8Br, 98%), (Poole, Dorset, UK). A variety of chemicals, including dichloromethane (CH_2Cl_2), deuterochloroform ($CDCl_3$), deuterium oxide (D_2O), ethanol (C_2H_5OH), potassium hydroxide (KOH), bis(acetonitrile)palladium dichloride ($PdCl_2(MeCN)_2$) and additionally, technical purity hexane (C_6H_{14}, 99%) and ethyl acetate ($C_4H_8O_2$, 99%) were bought from local markets. Schlenk line techniques were used to execute synthesis processes in an environment of nitrogen gases.

2.2. Instrumentation

HACH DR6000 RFID device was used for UV-Vis spectrophotometry measurement and Qiatek, FFP 4 devices were used for solid state conductivity measurement. Measurements were taken using a table-top press Model: YLJ-24 MTI Company, which can form pellets under 10 tons of pressure, and steel plates. For FT-IR measurements, measurements were taken with Bruker Tenson 27 device, and for thermogravimetric analysis, measurements were taken with TGA 400 (TGA-DTA) EXSTAR 6300 devices. In X-Ray diffraction (X-ray powder) analysis. Malvern Panalytical Empyrean device, and Electrothermal-9200 melting point device was used for the melting points of the products. Analysis on AGILENT brand ICP MS/MS 8800 Triple Quad ICP model device (Inductively Coupled Plasma), ^{1}H and ^{13}C-NMR analysis were performed using Varian As 300 Merkur spectrophotometer device, the results were recorded in $CDCl_3$ and D_2O solvents at vibration frequencies of 300 MHz and 75 MHz.

Thermogravimetric analysis was performed using a TGA 400 (TGA-DTA) EXSTAR 6300 instrument. A Malvern Panalytical Empyrean was used to perform X-ray diffraction (X-ray powder) analysis. Melting points of the compounds were measured using an Electrothermal-9200 melting point apparatus. FT-IR spectra of KBr pellets were recorded on an ATI Unicam 1000 spectrum, ^{1}H-NMR and ^{13}C-NMR spectra were recorded using a Varian As 300 Merkur spectrophotometer in $CDCl_3$ and D_2O at 300 MHz and 75 MHz, respectively.

The compounds (**3**), (**5**), (**6**), (**9**), (**10**), (**11**), and $IMe^{CNC}.2HPF_6$ were studied using cyclic and differential pulse voltammetry in DMF solvent at a concentration of 5 mM each, with 0.1 M nBu_4PF_6 serving as the supporting electrolyte in an inert atmosphere. A three-electrode cell linked to an external CHI 730C potentiostat powered by CHI software on a personal computer comprised the setup for the electrochemistry experiment. $Ag/AgNO_3$ (0.01 M) served as the reference electrode, while Pt wire served as a counter electrode [63]. The

working electrode was an electrode made from glassy carbon with a 0.5 mm diameter. In between experiments, every working electrode was thoroughly cleaned with a polishing pad and allowed to air dry. When reporting potentials versus $[Fe\text{-}(C_5H_5)_2]^+/[Fe(C_5H_5)_2]$, the measurement value versus $Ag/AgNO_3$ electrode is subtracted by 0.143 V.

2.3. Biological activity

2.3.1. Test organisms

In this study, minimal inhibition concentrations (MIC) were determined according to the CLSI (Clinical Laboratory Standards Institute) micro broth dilution method. To this end; **Gram positive bacteria:** *Bacillus cereus* (ATCC 14579), *Listeria monocytogenes* (ATCC 19115), **Gram negative bacteria:** *Escherichia coli* (ATCC 25922), *Salmonella thphimurium* (ATCC 14028), *Escherichia coli* (O157:H7), **Fungus:** *Candida albicans* (ATCC 10231), and **Antibiotic:** Ampicillin used. Fungal and bacterial strains were tested in sub-cultures using microorganisms that were acquired from Trakya University's Technology Research-Development Application and Research Center (TUTAGEM, Edirne, Turkey) [38].

2.3.2 Antibiotic control

The MIC values of compounds (**3**,**5**,**6**,**9**,**10**) were in the range of 50-100 µg µL for 1 strain in Gram-negative and Gram-positive bacteria and the control was not highly resistant to microorganisms. However, ampicillin was found to be very active even at the lowest concentration of 12.5 and killed the microorganisms in a short time. The antimicrobial activity of the Pd (II) complex showed similar activity compared to other metal complexes described in the literature [39].

2.3.3 Experimental setup

Five milliliters of sterilized LB broth have been measured in a sterilized tube. The tube holding the LB Broth solution was filled with a fixed volume (20 µL) of pure culture microorganisms in constant phase, including bacteria. At 37 °C, the mixture was cultivated for the entire night in an incubator with a shaking [40]. The next step was to mark the 3 mL sterilized solution of silver compound as A and transfer it to a 10 mL sterile tube. Next came the culture tube with 1 mL of a 3 mL Pd(II)-NHC compounds and 2 mL of LB Broth. After the solution was moved, serial dilution was carried out to produce a range of concentrations, and it was designated B. After the solution was moved, serial dilution was carried out to produce a range of concentrations, and it was designated B. A tube labeled C, which contained 2 mL of LB Broth, was filled with the well-agitated solution B (1 mL). For the D and E dilutions, the same procedure was carried out again. Ampicillin was employed as an antimicrobial control in cultures. A 0.45 µm sterile filters was used to filter stock solutions of soluble materials and antimicrobials. Cultures of bacteria and fungi were successfully inoculated. Every microplatelet was incubated for both 24 and 48 hours at 37 ˚C. At 600 nm, absorbance was measured, and vitality percentage values were calculated. All of the compounds' stock solutions were made in DMSO, and demineralized water was used to dilute them [41]. The tested compounds have been prepared at concentrations of 500, 250, 125, 62.5, 31.25, 15.56, 7.78 and 3.89 µM. After 24 and 48 hours of incubation, the results for both fungi and bacteria were evaluated on all inoculated plates. Minimum inhibition concentrations (MIC) were defined as the lowest concentrations of substances that inhibited growth.

2.3.4 Effect of solvent on antimicrobial activity

The broth dilution method is usually utilized to determine the MIC. The tested compound must be prepared in multiple dilutions in an appropriate solvent. The extracts need to be dried in order to gauge their antimicrobial activity. Even in the original solvent, it is frequently challenging to re-dissolve the extracts. Here, water can be used with solvents like methanol, ethanol, or DMSO. One of the most crucial elements that can influence in vitro

MIC measurement is the selection of an appropriate solvent. Since ethanol and DMSO [42] are miscible with water, they are recommended. Nonetheless, it has been documented that ethanol, DMSO, along other solvents utilized in different biological tests have antimicrobial properties. As a result, it is crucial to make sure that the organic solvent's ultimate concentration won't likely affect the biological test (MIC determination).

It should be mentioned that the sensitivity of each organism to these solvents may vary. In a 15% DMSO solution, the *Escherichia coli* bacteria's growth rate was stopped [43,44]. Based on this data, it was found that as DMSO concentrations increased, each microorganism's growth rates decreased [45].

2.4. Characterization and synthes methods

2.4.1. 2,2'-(([1,1'-biphenyl]-4,4'-diylbis(methylene))bis(oxy))dibenz aldehyde (3)

After adding 2-hydroxybenzaldehyde (**1**) (0.27 ml, 2.5 mmol) dropwise to the vial containing KOH (0.15g, 2.5 mmol) and ethanol (5 mL), 4,4'-bis(chloromethyl)-1,1'-biphenyl (**2**). The compound was added portionwise to the reaction medium as a solid (0.313 g, 1.25 mmol) over 1 hour. Backwashing was done at 78 degrees for 4 hours. The R_f values of the products against the starting materials on the TLC plate were evaluated under UV light to check whether products were formed and whether they were impurities. TLC chromatography [Ethyl acetate: Hexane (1:5)] method was used to finish the reaction. After the reaction was completed, the solid precipitate was filtered from water and crystallized. A vacuum oven was used to dry the resulting white crystals (scheme 1) [46-48].

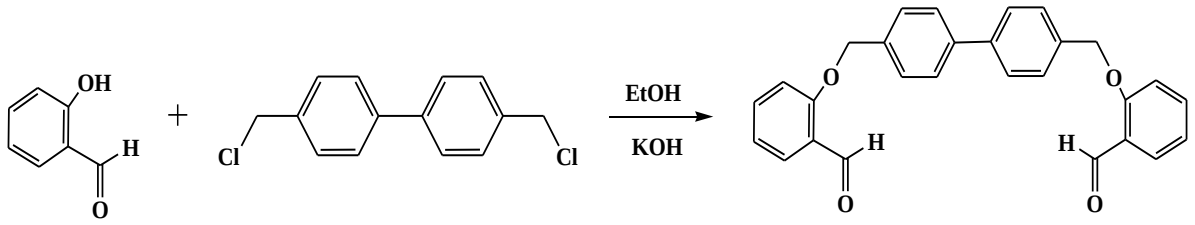

(**1**) (**2**) (**3**)

Scheme 1. The chemical structure of (3).

White solid. **Yield:** (0.45 g, % 86) **Mp.:** 195-198˚C. **Anal calc:** $C_{28}H_{22}O_4$, **LC-QTOF (m/z): cal:**422.4800, **found**: 422.4815 g/mol. **^{1}H-NMR** (300 MHz, $CDCl_3$): δ: 10.53 (s, 2H), 7.81 (dd, *J*=7.6 Hz, 4H), 7.62-7.52 (m, *J*=11.4-11.6 Hz 8H), 7.48 (t, *J*=10.4 Hz, 2H), 6.96 (t, *J*=5.8 Hz, 2H), 5.18 (s, 4H) ppm. **^{13}C-NMR** (75 MHz**,** $CDCl_3$): δ: 189.96 (C=O), 161.23, 140.83, 136.17, 131.56, 125.43, 121.33, 120.82, 113.25, 112.86, 106.25 (C=C), 70.42 (CH_2) ppm. **Ea.** (%) **cal.:** C: 79.60, H: 5.25, **found:** C: 79.55, H: 5.29. **IR(ATR)** (4000-450 cm^{-1}): 3000-2800 cm^{-1} υ(C-H), 1687 cm^{-1} υ(C=O), 1496 cm^{-1} υ (C=C). **UV-Vis** (λ max, (log ε) nm (~$M^{-1}cm^{-1}$): 206 (4.61), 256 (4.77), 303 (4.86) and 425 (4.80) nm. **ʌM** (DMSO, 10^{-3} M**,** 29.8 ºC**):** 3.6 µS/cm.

2.4.2. 2,2'-(([1,1'-biphenyl]-4,4'-diylbis(methylene))bis(oxy))bis(N-(prop-1-en-2-yl) aniline) (5)

After mixing KOH (500 mg, 9 mmol) in EtOH (15 mL) at 60 oC for 30 min, 2-acetamidophenol (**4**) (1.5g, 10 mmol) was added to the reaction flask, and the color changed to dark green. After stirring for 1 hour, 4,4'-bis(chloromethyl)-1,1'-biphenyl (**2**) (1g, 4 mmol) was added piecemeal for 1 hour. The mixture was stirred at 60-70 °C for 24 hours. The solvent was evaporated in a rotary evaporator and the remaining part was washed with 500 mL of cold water. After this process was repeated twice, the precipitated part was filtered with filter paper (scheme 2).

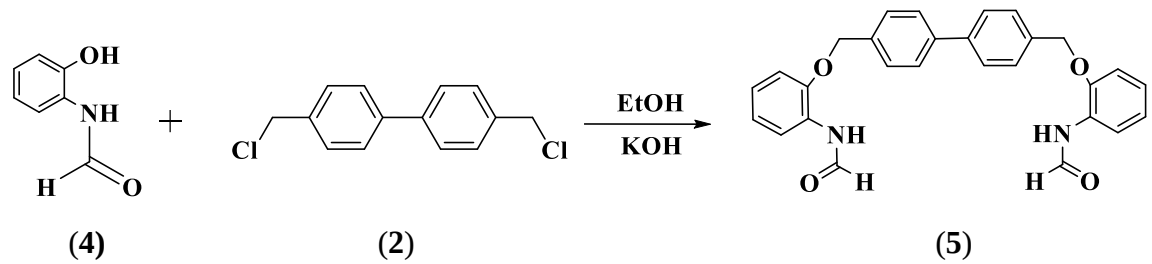

(**4**) (**2**) (**5**)

Scheme 2. The chemical structure of (**5**).

Cream solid. **Yield:** (1.69 g, % 88). **Mp.:** 195-198˚C. **Anal calc:** $C_{30}H_{28}N_2O_4$, **LC-QTOF (m/z): cal:**480.2200, **found:** 480.2551 g/mol (0.45g), **^{1}H-NMR** (300 MHz, $CDCl_3$) 2.2 (s, 6H, CH_3), 5.2 (s, 4H, CH_2), 6.9–7.8 (m, *J*=10.6-10.8 Hz 16H), 8.4(s, 2H, NH) ppm. **^{13}C-NMR** (75 MHz**,** $CDCl_3$): 25.7 (CH_3), 71.3 (CH_2), 112.3, 120.7, 122.2, 124.3, 128.1, 128.8, 128.9, 136.3, 141.3, 147.5, 168.9 (C=O) ppm. **E A** (%) **cal.:** C: 74.98, H: 5.87, N, 5.83, **found:** C: 74.95, H: 5.89, N: 5.87. **IR(ATR)** (4000-450 cm^{-1}): 3294 ν(NH), 3070–3037 ν(C≡C–H), 2943–2844 $\nu_{as}(CH_3)$, $\nu_s(CH_3)$, $\nu_{as}(CH_2)$, $\nu_s(CH_2)$, 1657 ν(C=O), 1597 ν(C≡C), 1257 ν(C–O). **UV-Vis** (λ max, (log ε) nm (~$M^{-1}cm^{-1}$): 235 (4.54), 295 (4.89), 357 (4.88) and 419 (3.47) nm. **ʌM (**DMSO, 10^{-3} M, 29.8 ºC)**:** 4.1 µS/cm.

2.4.3. 2,2'-(([1,1'-biphenyl]-4,4'-diylbis(methylene))bis(oxy))dianiline (6)

NaOH dissolved in 10 mL of pure water (11 times) was added into 30 mL of ethanol and mixed at room temperature in the reaction flask (**5**). The mixed suspension was refluxed at 110 °C for 1 week. After TLC control showed that the starting material was completely consumed, the mixture in the reaction flask was washed with 500 mL of pure water. Washing with 250 mL of water was repeated 5 times, then the whitish solid was filtered by vacuum filtration and dried in vacuum (scheme 3).

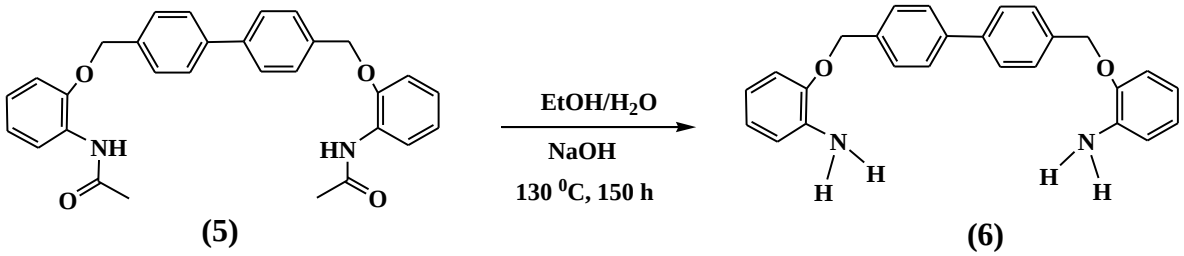

(**5**) (**6**)

Scheme 3. The chemical structure of (**6**).

Whitish solid. **Yield:** (1.69 g, 36%). **Mp.:** 199-202˚C. **Anal calc:** $C_{30}H_{28}N_2O_4$, **LC-QTOF (m/z): cal:**480.2200, **found:** 480.2551 g/mol (0.45g), **^{1}H-NMR** (300 MHz, $CDCl_3$) 3.9 (s, 4H, NH_2), 5.1 (s, 4H, CH_2), 6.7–7.6 (m, 16H) ppm. **^{13}C-NMR** (75 MHz**,** $CDCl_3$): 70.3 (CH_2), 112.3, 115.5, 118.7, 121.8, 127.6, 128.4, 136.6, 136.7, 140.7, 146.7(C=C, aromatic) ppm. **Ea.**(%) **cal.:** C: 77.76, H: 6.10, N: 7.07, **found:** C: 77.80, H: 6.16, N: 7.09. **IR(ATR)** (4000-450 cm^{-1}): 3516, 3365(NH_2), 3066–3037 (C≡C–H), 2923–2867 (CH_2), 1607 ν(C≡C), 1208(C–O). **Q-TOF (m/z):** $[M+H]^+$ **cal.**: 396.1800, **found:** 396.1911. **UV-Vis** (λ max, (log ε) nm (~$M^{-1}cm^{-1}$): 239 (4.68), 302 (4.48), 368 (4.35), 434 (4.69) and 515 (4.99) nm. **ʌM** (DMSO, 10^{-3} M, 29.8 ºC)**:** 4,94 µS/cm.

2.4.4. 2,2'-((1,2-phenylenebis(methylene))bis(sulfanediyl))dianiline (9)

KOH (0.2 g, 3.8 mmol) was added to the two-necked flask containing ethanol (5 mL) and stirred for 1 hour at room temperature. 2-aminothiophenol (**7**) compound (0.476 g, 3.8 mmol) diluted with ethanol was added dropwise to the reaction medium for 1 hour. Then, 1,2-

bis(bromomethyl)benzene (**8**) compound (0.5 g, 1.9 mmol) dissolved in ethanol was added slowly to the mixture within 1 hour. Backwashing was done for 24 hours and the reaction was terminated by checking with TLC [Ethyl acetate: Hexane (1:5)]. The solid precipitate formed at the end of the reaction was filtered and crystallized in water. The light brown crystals formed were dried in a vacuum oven (scheme 4).

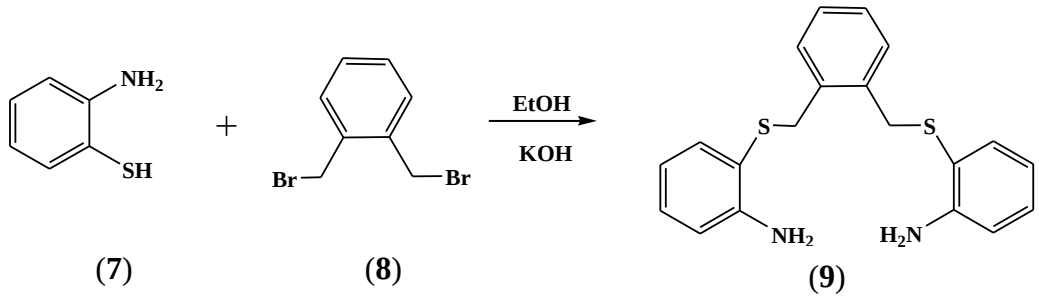

(**7**) (**8**) (**9**)

Scheme 4. The chemical structure of (**9**).

Light brown solid. **Yield:** (0.45 g, 65%). **Mp.:** 89-92˚C. **Anal calc:** $C_{20}H_{20}N_2S_2$, **Q-TOF (m/z):** $[M+H]^+$ 352.5100, found: 352.5247 g/mol. Mp: 89-92ºC. **IR(ATR)** (4000-450 cm^{-1}): 3445,3350 cm^{-1} υ(N-H), 3070-2910 cm^{-1} υ(C-H), 1603 cm^{-1} υ(C=C), 1018 cm^{-1} υ(Ar-S-Ar). **^{1}H-NMR** (300 MHz, $CDCl_3$): δ: 7.28 (d, J = 2.6 Hz, 2H), 7.24 – 7.07 (m, 3H), 7.01 (d, J = 3.2 Hz, 2H), 6.78-6.65 (m, 3H), 6.63 (t, J = 6.9 Hz, 2H), 4.30 (s, 4H), 3.99 (s, 4H). **^{13}C-NMR** (75 MHz, $CDCl_3$): δ: 148.94 (C), 136.85, 136.46, 130.78, 130.41, 127.58, 118.71, 117.54, 115.11 (C), 36.90 (CH_2). **Ea.**(%) **cal.:** C: 77.95, H: 5.61, N: 3.71, **found:** C: 77.98, H: 5.68, N: 3.75. **UV-Vis** (λ max, (log ε) nm (~$M^{-1}cm^{-1}$): 255 (4.64), 297 (4.93), 381 (4.81), 447 (4.06) and 498 (4.91) nm. **ʌM** (DMSO, 10^{-3} M, 29.8 ºC)**:** 3.4 µS/cm.

2.4.5.(6Z,15Z)-4,18-dioxa-9,13-dithia-7,15-diaza-1,2(1,4),5,8,11,14,17(1,2)-heptabenzen acyclononadecaphane-6,15-diene (10)

2,2'-(([1,1'-biphenyl]-4,4'-diylbis(methylene))-bis(oxy))dibenzaldehyde (**3**) (0.14 g, 0.33 mmol) was added to the flask containing 10 ml of ethanol and It was dissolved by applying heat. Then, 2'-((1,2-phenylenebis(methylene))bis(sulfandiyl))dianiline (**9**) (0.116 g, 0.33 mmol) was dissolved in 5 ml of ethanol and added slowly and reflux for 4-5 hours. Yellow crystals precipitated. The crystals filtered through blue banded filter paper were washed with ethanol and allowed to dry (scheme 5).

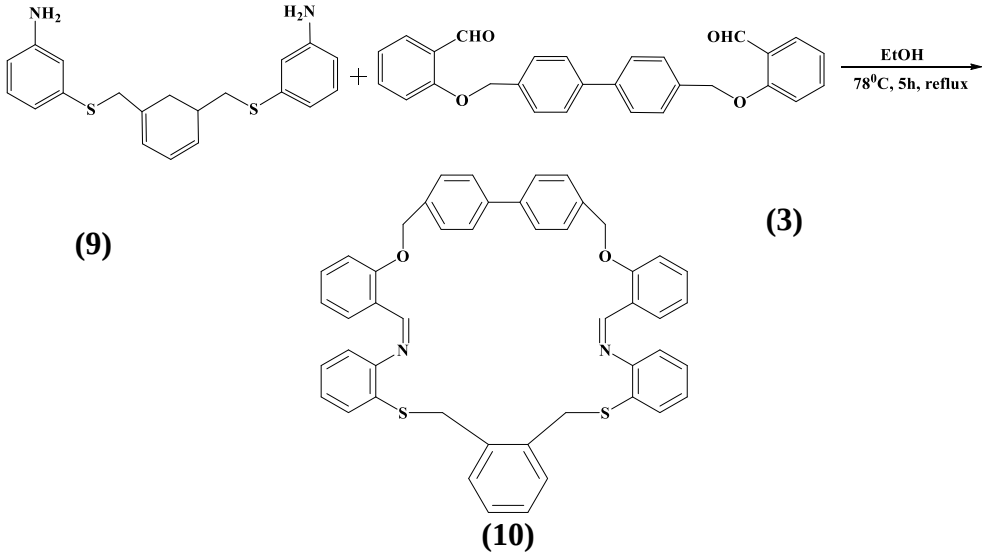

(**9**) (**3**) (**10**)

Scheme 5. The chemical structure of (**10**).

Brown solid. **Yield:** (0.45 g, 62%). **Mp.:** 89-92˚C. **Anal calc:** $C_{48}H_{38}N_2O_2S_2$, **Q-TOF (m/z):** $[M+H]^+$ **calc:**738,2400, **found:** 738,2412 g/mol. Mp: 89-93 ºC. **IR(ATR)** (4000-450 cm^{-1}): 3445,3350 cm^{-1}υ(N-H), 3070-2910 cm^{-1} υ(C-H), 1603 cm^{-1} υ(C=C), 1018 cm^{-1} υ(Ar-S-Ar). **^{1}H-NMR** (300 MHz, $CDCl_3$): δ: 8.57 (s, J = 2.6 Hz, 4H), 7.82 (d, J = 2.6 Hz, 2H), 7.11 – 7.54 (m, 3H), 7.04 (d, J = 3.2 Hz, 2H), 5.21 (s, J = 9.6 Hz, 8H), 4.15 (s, 8H). **^{13}C-NMR** (75 MHz, $CDCl_3$): δ: 140.03 (C), 139.78, 137.51, 134.48, 132.48, 131.97, 128.16, 127.63, 127.18, 125.62, 124.28, 121.86, 114.05, 117.08, 78.08 (C), 38.52 (CH_2). **Ea.**(%) **cal.:** C: 78.02, H: 5.18, N: 3.79, **found:** C: 78.09, H: 5.24, N: 3.75. **UV-Vis** (λ max, (log ε) nm (~$M^{-1}cm^{-1}$): 265 (4.58), 304 (4.98), 391 (4.84), 453 (4.52) and 518 (4.16) nm. **ʌM** (DMSO, 10^{-3} M, 29.8 ºC): 5.1 μS/cm.

2.4.6.(6Z,15Z)-4,18-dioxa-9,13-dithia-7,15-diaza-1,2(1,4),5,8,11,14,17(1,2)-heptabenzen acyclononadecaphane-6,15-diyliene palladium (II) chloride (11)

(6*Z*,15*Z*)-4,18-dioxa-9,13-dithia-7,15-diaza-1,2(1,4),5,8,11,14,17(1,2)-heptabenzen acyclononadecaphane-6,15-diene (**10**) (0.243 g, 0.33 mmol) was added to the flask containing 10 ml of ethanol and it was dissolved by applying heat. Then, one of $PdCl_2(MeCN)_2$ (0.085 g, 0.33 mmol) was dissolved in 5 ml of ethanol was added and backwashed for half an hour. Afterward, 2'-((1,2-phenylenebis(methylene))bis(sulfandiyl)) dianiline (**9**) (0.116 g, 0.33 mmol) was dissolved in 5 ml of ethanol and added slowly and reflux for 4-5 hours. Light brown crystals precipitated in the Pd^{2+} complex. The crystals were filtered through blue banded filter paper, washed with ethanol, and allowed to dry (scheme 6) [49].

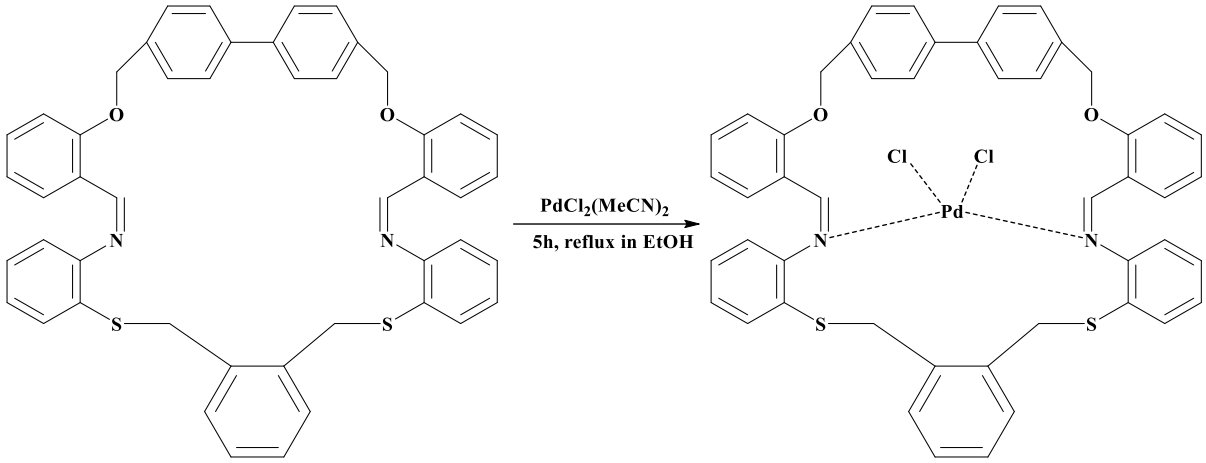

(10) **(11)**

Scheme 6. The chemical structure of (**11**).

Brown solid. **Yield:** (0.35 g, % 62). **Mp.:** 89-92˚C. **Anal calc:** $C_{48}H_{38}Cl_2N_2O_2PdS_2$, **Q-TOF (m/z):** $[M+H]^+$ **calc:** 916.2800, **found:** 916.2815 g/mol. Mp: 96-99 ºC. **IR(ATR)** (4000-450 cm^{-1}): 3445-3350 cm^{-1}υ(N-H), 3070-2900 cm^{-1} υ(C-H), 1610-1630 cm^{-1} υ (CH=N), 1599 cm^{-1} υ (C=C), 1018 cm^{-1} υ(Ar-S-Ar). **^{1}H-NMR** (300 MHz, $CDCl_3$): δ: 8.57 (s, J = 2.6 Hz, 4H), 7.82 (d, J = 2.6 Hz, 2H), 7.11 – 7.54 (m, 3H), 7.04 (d, J = 3.2 Hz, 2H), 5.21 (s, J = 9.6 Hz, 8H), 4.15 (s, 8H). **^{13}C-NMR** (75 MHz, $CDCl_3$): δ: 140.03 (C), 139.78, 137.51, 134.48, 132.48, 131.97, 128.16, 127.63, 127.18, 125.62, 124.28, 121.86, 114.05, 117.08, 78.08 (C), 38.52 (CH_2). **Ea.**(%) **cal.:** C: 62.92, H: 4.18, N: 3.06, **found:** C: 62.99, H: 4.24, N: 3.05. UV-Vis (λ max, (log ε) nm (~$M^{-1}cm^{-1}$): 225 (4.30) nm and 300 (4.47) show **π → π*** transition, and peaks at 558 (5.04), 650 (4.98) and 691 (4.79) nm are the LCMT (**n → π***) transition, ICP (Ag): Calc.: 12.14, Found: 12.19%. **ʌM** (DMSO, 10^{-3} M, 29.8 ºC): 111.27 μS/cm. **μeff** (BM, 24 ºC)**:** 0.1 BM.

3. Results and discussion

3.1. FTIR spectra

In the FTIR spectrum of (**3**), it is 3000-2800 cm^{-1} C-H peaks belonging to the aromatic ring, a sharp C=O peak belonging to the aldehyde group at 1687 cm^{-1}, and a C=C peak belonging to aromaticity at 1595 cm^{-1} were observed.

For (**6**), there is the characteristic N-H peak at 3294 cm^{-1}, the aromatic ring and aliphatic C-H peaks between 3080-2800 cm^{-1}, the sharp C=O peak of the carbonyl at 1656 cm^{-1} and the peak at 1598 cm^{-1}. The C=C peak belonging to aromaticity was observed at (**1)**, and the C-O peak was observed at 1257 cm^{-1}.

For (**7**), the amine N-H characteristic peak at 3516 and 3365 cm^{-1}, the aromatic ring and aliphatic C-H peaks between 3080-2800 cm^{-1}, and the C=C peak belonging to aromaticity at 1607 cm^{-1}, C-O peaks are seen around 1208 cm^{-1}.

For (**9**), N-H peaks belonging to NH_2 at 3445-3350, 3070 cm^{-1}. C-H peaks belonging to the aromatic ring are seen between 2910 cm^{-1}, C=C peak belonging to the aromatic ring at 1603 cm^{-1} and Ar-S-Ar peak belonging to the structure at 1018 cm^{-1}.

For (**10**), N-H peaks belonging to NH_2 at 3455-3360, 3075 cm^{-1}. C-H peaks belonging to the aromatic ring are seen between 2912 cm^{-1}, C=C peak belonging to the aromatic ring at 1607 cm^{-1} and Ar-S-Ar peak belonging to the structure at 1022 cm^{-1}.

For (**11**), N-H peaks belonging to NH_2 at 3468-3371, 3079 cm^{-1}. C-H peaks belonging to the aromatic ring are seen between 2915 cm^{-1}, C=C peak belonging to the aromatic ring at 1608 cm^{-1} and Ar-S-Ar peak belonging to the structure at 1023 cm^{-1}.

3.2. NMR spectra

In the ^{1}H-NMR spectrum of (**3**), the peak CH_2 indicated by n is at 5.18 ppm. The hydrogen peak belonging to is singlet and its integral is 4. The integral of the peak of the aromatic ring marked d at 5.18 and 6.96 ppm is 2 and triplet. The integral of the peak at 5.18 and 6.96 ppm 7.48 ppm, indicated by e and belonging to the aromatic ring, is 2 and triplet. The integral of the aromatic peaks belonging to the biphenyl group, denoted by between 7.62-7.52 ppm is 8 and multiplet. At 7.81 ppm, the integral of the peaks belonging to the aromatic ring marked is 4 and they are the doublet of the doublet. The a peak at 10.53 ppm, which belongs to the aldehyde, is singlet and its integral is 2. In the ^{13}C-NMR spectrum of (**3**), the peaks belonging to the benzene ring and biphenyl group are 161.23, 161.23, respectively. They appear at 140.8, 136.1, 135.5, 125.4, 121.3, 120.8, 113.2, 112.8, 106.2 ppm. The peak belonging to the carbonyl group is seen at 189.9 ppm, and the peak belonging to the CH_2 carbon and indicated by n is seen at 70.4 ppm. The peak belonging to the carbonyl group is seen at 189.9 ppm, and the peak belonging to the CH_2 carbon and indicated by n is seen at 70.4 ppm.

For (**5**), it is a proton singlet with an integral of 6 belonging to CH_3 bonded to carbonyl at 2.23 ppm. The peak at 5.24 ppm is the hydrogen peak of CH_2, which is bound to oxygen, and its integral is 4 and singlet. The multiplet peaks with an integral of 16 between 6.96-7.86 ppm belong to the aromatic ring. At 8.4 ppm, the NH proton is singlet and its integral is 2. In the ^{13}C-NMR spectrum of compound (**5**) is examined, the peak of CH_3 bound to carbonyl is at 25.7 ppm, the peak of CH_2 bound to oxygen is at 71.3 ppm, 112.3, 120.7, 122.2, 124.3, 128.1, 128.8, 128.9, 136.3. A total of 13 carbon peaks were observed, including 10 aromatic carbon peaks at 141.3, 147.5 ppm and carbonyl carbon at 168.9 ppm. Disappearance of the broad OH peak around 3500 cm^{-1} in the FTIR spectrum, shift of chlorine-bound CH_2 protons at 4.7 ppm in ^{1}H-NMR spectrum of (**5**) to 5.24 ppm, ^{13}C-NMR The fact that a total of 13 carbons are seen in the NMR spectrum shows that the targeted structure has been obtained. The appearance of the C=O peak at 1687 cm^{-1} in the FTIR spectrum, the disappearance of the singlet O-H peak at 11.02 ppm belonging to the salicyl aldehyde compound in the ^{1}H-NMR spectrum, the shift of the singlet peak belonging to the carbonyl hydrogen at 9.88 ppm to

10.53 ppm. The shift of the CH_2 peak belonging to the compound (**3**) from 4.68 to 5.18 ppm, the CH_2 peak at 70.42 ppm in the ^{13}C-NMR spectrum, the C=O peak at 189.69 ppm and a total of 12 carbons The appearance of peaks proves that the structure has formed.

For (**6**), it see the singlet NH_2 peak at 3.95 ppm, and the peak at 5.19 ppm is the hydrogen peak belonging to CH_2 bound to oxygen, and its integral is 4 and singlet. Multiplet peaks with an integral of 16 between 6.79 and 7.68 ppm belong to aromatic rings. In the ^{13}C-NMR spectrum of the compound (**6**), 10 carbon peaks are seen at 70.3 ppm (CH_2), 112.3, 115.5, 118.7, 121.8, 127.6, 128.4, 136.6, 136.7, 140.7, 146.7, aromatic. In the FTIR spectrum, the characteristic NH_2 peak occurs at 3516 and 3365 cm^{-1}, and the carbonyl peak at 1656 cm^{-1} disappears. The disappearance of the carbonyl-bound CH_3 peak at 2.23 ppm in the ^{1}H-NMR spectrum and the formation of a singlet NH_2 peak at 3.95 ppm, the disappearance of the peak showing the carbonyl carbon at 168.4 ppm in the ^{13}C-NMR spectrum and the observation of a total of 11 carbon peaks parallel to the expected structure indicate that the structure has been formed.

For (**9**) in the ^{1}H-NMR spectrum, peak 1 at 4.30 ppm is the hydrogen peak of NH_2, a singlet, with an integral of 4. Peak number 8 at 3.99 ppm is the hydrogen peak of the CH_2, singlet and its integral is 4.30 and 5 are bonded to the aromatic ring where NH_2 is located, and their integrals are 2. They are double and triple respectively. The integrals of peaks 4 and 6 are 2 and are triplet and double, respectively. The integrals of peaks 10 and 11 are 2 and multiple. In the ^{13}C-NMR spectrum, the peaks belonging to the benzene ring are 2,9,6,4,10,11,7,5,3 and are at 148.9, 136.8, 136.4, 130.7, 130.4, 127.5, 118.7, 117.5, 115.1 ppm respectively. Peak number 8 belonging to CH_2 carbon is seen at 36.90 ppm. In the FTIR spectrum, the N-H peaks of NH_2 are seen at 3350 and 3345 cm^{-1}, in the ^{1}H-NMR spectrum, the singlet S-H peak of the (**7**) compound disappears at 2.94 ppm and the singlet peak disappears at 2.94 ppm. NH_2 at 4.2 ppm disappears at 4.3 ppm. The shift of the CH_2 peak of the compound (**8**) from 4.68 ppm to 3.99 ppm, the shift of the CH_2 peak to 36.90 ppm in the ^{13}C-NMR spectrum, and the appearance of the following peaks: 11 carbons in total Its presence proves that the structure was formed.

For (**10**) in the ^{1}H-NMR spectrum, peak 1 at 4.15 ppm is the hydrogen peak of NH, a singlet, with an integral of 4. Peak number 8 at 5.21 ppm is the hydrogen peak of the CH_2, singlet and its integral is 4.30 and 5 are bonded to the aromatic ring where NH_2 is located, and their integrals are 2. They are double and triple respectively. The integrals of peaks 4 and 6 are 2 and are triplet and double, respectively. The integrals of peaks 10 and 11 are 2 and multiple. Multiplet peaks with an integral of 16 between 7.04 and 7.11–7.54 ppm belong to aromatic rings, the shift of the singlet peak belonging to the carbonyl hydrogen at 8.57 ppm. In the ^{13}C-NMR spectrum, the peaks belonging to the benzene ring are 2,9,6,4,10,11,7,5,3 and are at 140.03, 139.78, 137.51, 134.48, 132.48, 131.97, 128.16, 127.63, 127.18, 125.62, 124.28, 121.86, 114.05, 117.08, 78.08, 38.52 ppm respectively. Peak number 8 belonging to CH_2 carbon is seen at 36.90 ppm. In the FTIR spectrum, the N-H peaks of NH_2 are seen at 3350 and 3345 cm^{-1}, in the ^{1}H-NMR spectrum, the singlet S-H peak of the (**7**) compound disappears at 2.94 ppm and the singlet peak disappears at 2.94 ppm. NH_2 at 4.2 ppm disappears at 4.3 ppm. The shift of the CH_2 peak of the compound (**8**) from 4.68 ppm to 3.99 ppm, the shift of the CH_2 peak to 36.90 ppm in the ^{13}C-NMR spectrum, and the appearance of the following peaks: 11 carbons in total Its presence proves that the structure was formed.

For (**10**) and (**11**) in the ^{1}H-NMR spectrum are same peaks. In the ^{13}C-NMR spectrum, the peaks belonging to the benzene ring are 2,9,6,4,10,11,7,5,3 and are at 140.0, 139.7, 137.5, 134.4, 132.4, 131.9, 128.1, 127.6, 127.1, 125.6, 124.2, 121.8, 114.0, 117.0, 78.0, 38.5 ppm respectively. Peak number 8 belonging to CH_2 carbon is seen at 36.90 ppm. In the FTIR spectrum, the N-H peaks of NH_2 are seen at 3350 and 3345 cm^{-1}, in the ^{1}H-NMR spectrum, the singlet S-H peak of the (**7**) compound disappears at 2.94 ppm and the singlet peak disappears at 2.94 ppm. NH_2 at 4.2 ppm disappears at 4.3 ppm. The shift of the CH_2 peak of the compound (**8**) from 4.68 ppm to 3.99 ppm, the shift of the CH_2 peak to 36.90 ppm in the

^{13}C-NMR spectrum, and the appearance of the following peaks: 11 carbons in total Its presence proves that the structure was formed (table 1).

^{1}H NMR (ppm)						
(3)	5.18	6.96	7.48	7.62 7.52	7.81	10.53
(5)	2.23	5.24	6.96	7.86	9.88 10.53	11.02
(6)	3.95	5.19	6.79	7.68	-	-
(9)	3.99	4.30	-	-	-	-
(10)	4.15	5.21	7.04 7.11 7.54	7.82	8.57	-
(11)	4.15	5.21	7.04 7.11 7.54	7.82	8.57	-

^{13}C NMR (ppm)						
(3)	70.4	106.2	112.8 113.2	125.4 121.3 120.8	136.1 135.5 140.8	161.2 161.2
(5)	71.3	112.3	120.7 122.2 124.3	128.1 128.8 128.9	136.3 141.3	168.9
(6)	70.3	112.3 115.5 118.7	121.8 127.6 128.4	136.6 136.7	140.7 146.7	-
(9)	-	115.1 117.5 118.7	127.5	130.4 130.7	136.8 136.4	148.9
(10)	38.5 78.0	114.0 117.0	125.6 124.2 121.8 128.1 127.6 127.1	134.4 132.4 131.9	139.7 137.5	140.0
(11)	38.5 78.0	114.0 117.0	128.1 127.6 127.1 125.6 124.2 121.8	134.4 132.4 131.9	139.78, 137.51	140.0

Table 1. NMR Spectra of Compounds

3.3. TGA-DTA measurement

Thermal gravimetric analysis (TGA) measurements of synthesized Paladium and palladium-containing metal complexes were presented in supplementary materials. Depending on the weight loss of the complexes, organic and inorganic parts were distinguished from each other. This weight loss takes place in three steps. In the 1st step, the moisture of water molecules were removed from the molecules the temperature between 101 and 297 °C. In the 2nd step, there is a weight loss between 298 and 437 °C, depending on the carbonization of the metal complexes. In the 3rd step, the carbonization of the organic part in the metal complexes was continued the temperature between 437 and 1000 °C. In addition, the highest weight loss was occured in the last step. The thermogravimetric analysis results

indicate that the molecular weight ratio of PdO and Pd is compatible with the proposed structure.

3.4. Magnetic moment measurements

All complexes showed an effective magnetic moment of zero, or μeff, which is indicative of the diamagnetic square planar d^8 Pd(II) system in the absence of unpaired electrons. The complexes' molar conductivity of 0 $\lambda_m/\Omega^{-1}cm^2/mol$ and lack of counterions suggested that they were not electrolytic.

3.5. Powder PXRD measurements

X-ray analysis is crucial for examining organic compounds, where elements like nitrogen, hydrogen, and carbon play key roles, while structural stability is influenced by components such as halides and other stabilizing ions [50-55]. The PXRD peaks for (**3**) are at 5.25, 15.15, 79.60º, for (**5**) are at 2θ=5.87, 5.83, 13.32, 74.98º, for (**6**) are at 2θ=6.10, 7.07, 8.07, 78.76º, for **(9)** are at 2θ= 5.72, 7.95, 18.19, 50.12, 68.14º, for (**10**) 2θ= 3.65; 4.17, 5.52, 8.36, 78.30º, and for (**11**) were observed at 2θ=2.97, 3.39, 4.48, 6.79, 7.51, 11.27, and 63.59º. It may be due to the wide form of halogen and organic ligands around 8-28°.

3.6. Electronic spectra

In the electronic spectrum of organic structure compounds (**3**), (**5**), (**6**), (**9**) and (**10**), it has two absorption bands at 206 nm (ε = 461 L/molxcm), assigned to **π-π*** transitions at 256 nm (ε = 477 L/molxcm) and 303 nm (ε = 486 L/molxcm) and n- at 384 nm (ε = 960 L/molxcm), 385 nm (ε = 1030 L/molxcm) and 425 nm π* transitions (ε = 980 L/molxcm), respectively. For (**3**) 206 nm (ε = 461 L/molxcm), 256 nm (ε = 477 L/molxcm), 303 nm (ε = 486 L/molxcm), 425 nm (ε = 480 L/molxcm), for (**5**) and 235 (ε = 454 L/molxcm), 295 (ε = 489 L/molxcm), 357 (ε = 488 L/molxcm), 419 (ε = 347 L/molxcm), for (**6**) molxcm), 606 (ε = 1460 L/molxcm) and 305 nm (ε = 340 L/molxcm), for (**6**) and 239 (ε = 468 L/molxcm), 302 (ε = 448 L/molxcm), 368 (ε = 435 L/molxcm), 434 (ε = 469 L/molxcm), 515 (ε = 499 L/molxcm), for (**9**) 255 nm (ε = 464 molxcm), 297 (ε = 493 L/molxcm), 381 (ε = 481 L/molxcm), 447 (ε = 406 L/molxcm), 498 (ε = 491 L/molxcm), for (10) 265 nm (ε = 458 molxcm), 304 (ε = 498 L/molxcm), 391 (ε = 484 L/molxcm), 453 (ε = 452 L/molxcm), 518 (ε = 416 L/molxcm), for (**11**) 225 nm (ε = 430 molxcm), 300 (ε = 447 L/molxcm), **π → π*** transition, 558 (ε = 504 L/molxcm), 650 (ε = 498 L/molxcm), 691 (ε = 479 L/molxcm), LCMT (**n → π***) transition, which are assigned to the transitions $^1\mathbf{A_{1g}} \rightarrow {}^1\mathbf{A_{2g}}$, $^1\mathbf{A_{1g}} \rightarrow {}^1\mathbf{B_{1g}}$ and $^1\mathbf{A_{1g}} \rightarrow {}^1\mathbf{Eg}$, respectively.

The absorbances observed at between 206 and 304, nm represents the transition charge transfer from the nitrogen atom to the Pd^{2+} ion in the Schiff base. According to the electronic spectrum results, the synthesized palladium complex has a square planar geometry in which it is coordinated by the central Pd^{2+} ion. The electronic spectrum of the Pd(II) complex (**11**) shows three absorption bands in the range of 558, 650 and 691 nm.

3.7. ICP-MS analysis

Using combined solvent extraction and anion exchange preconcentration techniques along with isotope dilution, it is possible to separate Pd from the same sample. In other analyses, the organic part of the Schiff base was analyzed very positively by analytical methods and compared with the literatüre.

3.8. Analysis of conductivity and resistance

When the ^1H and ^{13}C-NMR results of Pd(II) complex (**11**) were examined, it gave similar results to the complex with [1+1] or [2+2] ratio. No nitrogen resonance indicating chemical equivalence of this ligand could be detected in the NMR spectra of any other compound in a similar solution. This was confirmed by the fact that the NMR spectra of the

ligand showed no discernible resonance and their molar conductivity in aqueous solutions was very low (<1 S cm^2/mol).

Conductivity measurements of the synthesized compounds were taken at a molar concentration of 10^{-3} M in DMF medium. The conductivity values of the compounds (**3**), (**5**), (**6**), (**9**) and (**10**), which are 1:1 electrolyte, were determined as 11.75, 21.48, 27.75 and 31.49 μS/cm, respectively. The conductivity values of the Pd^{2+} complex was determined to increase to 111.27 μS/cm, indicating that they are [1+1] electrolytes, respectively.

Solid-state conductivity measurements of the compounds (**3**), (**5**), (**6**), (**9**) and (**10**) were measured with a four-point probe device. All materials were pressed into pellet form using a pellet machine. The highest conductivity was obtained as 529 μS×cm^{-1} for the Pd(II) complex. Other conductivity results are 47.8, 57.42, 68.71 and 96.45 μS×cm^{-1} for (**3**), (**5**), (**6**), (**9**) and (**10**), respectively. There were similar relationships between the conductivity results obtained in liquid form and solid-state form. It has a higher conductivity result for the Pd(II) complex, with values of 529 μS/cm. Including Pd^{2+} ions in the complex form increases the conductivity results.

The [1+1] electrolyte conductivity for (**11**) shows that there are no metallophilic interactions in the DMF solution. Parallel to the 50% more ions in the DMF solution, the Pd(II) complex (**11**) exhibits higher conductivity than the ligands, (**3**), (**5**), (**6**), (**9**) and (**10**). At 1 mM concentrations of 1, 2, and 3, respectively, the calculated molar conductance (ΛM) values of 354 μS/cm fall within the expected ΛM range for a 2:1 electrolyte in DMF. The increased solubility of the complexes in polar solvents is responsible for the remarkable increase in current in the mixture of DMF and CH_2Cl_2 (1:7). Electrical resistance between two copper electrodes one centimeter apart was measured by passing a voltage through a constant DC source with a current range of one milliampere and a frequency range of 1000 Hertz.

3.9. Antimicrobial activities

The measurement of the antibacterial activity of six different compounds was tested on four different bacterial and one yeast species [50]. The average results of the three repeated tests are given separately in table 2. The antimicrobial activities of Pd(II)-NHC complexes showed that they possessed a very broad spectrum of antimicrobial activity. Based on the corresponding molar mass of the samples, the MIC values in the normality unit (μg/mL) were directly converted to MIC values in the molarity unit [50].

Samples	**Gram-negative bacteria**		**Gram-positive bacteria**		**Fungi**
	Escherichia coli (Mean±SE)	***Listeria monocytogenes*** (Mean±SE)	***Stapylococcus aureus*** (Mean±SE)	***Bacillus cereus*** (Mean±SE)	***Candida albicans*** (Mean±SE)
(**3**)	75.96±0.11	78.08±0.12	80.23±0.14	80.74±0.11	85.69±0.13
(**5**)	72.81±0.17	75.69±0.13	80.24±0.15	81.39±0.14	82.74±0.15
(**6**)	76.39±0.11	78.08±0.13	80.25±0.19	80.74±0.16	85.69±0.13
(**9**)	66.74±0.13	67.34±0.13	70.41±0.08	70.84±0.09	80.74±0.13
(**10**)	48.85±0.17	49.62±0.14	80.27±0.21	80.74±0.18	85.69±0.18
(**11**)	11.25±0.14	12.48±0.15	14.38±0.17	14.96±0.11	13.78±0.15
Ampicillin	0.72±0.01	0.74±0.00	0.68±0.01	0.69-0.01	0.24±0.01

Table 2. MIC values for compounds in antimicrobial tests.

Compounds (**3**), (**5**), (**6**), (**9**), (**10**), and (**11**) have inhibitory effects against four different bacteria *Escherichia coli* O157: H7 (ATCC 25922), *Listeria monocytogenes* (ATCC 19115), *Staphylococcus aureus* (ATCC 25923), *Bacillus cereus* (ATCC 11778) and against one type of fungus *Candida albicans* (ATCC 10231), on the other hand they have a very low inhibitory effect on different properties of bacterial species and fungi, with much lower antimicrobial activity compared to the drug ampicillin, in the indicated absorbance measurements. It is slightly more effective against bacteria and fungi, although there are some statistical flaws (figure 9) [51,52].

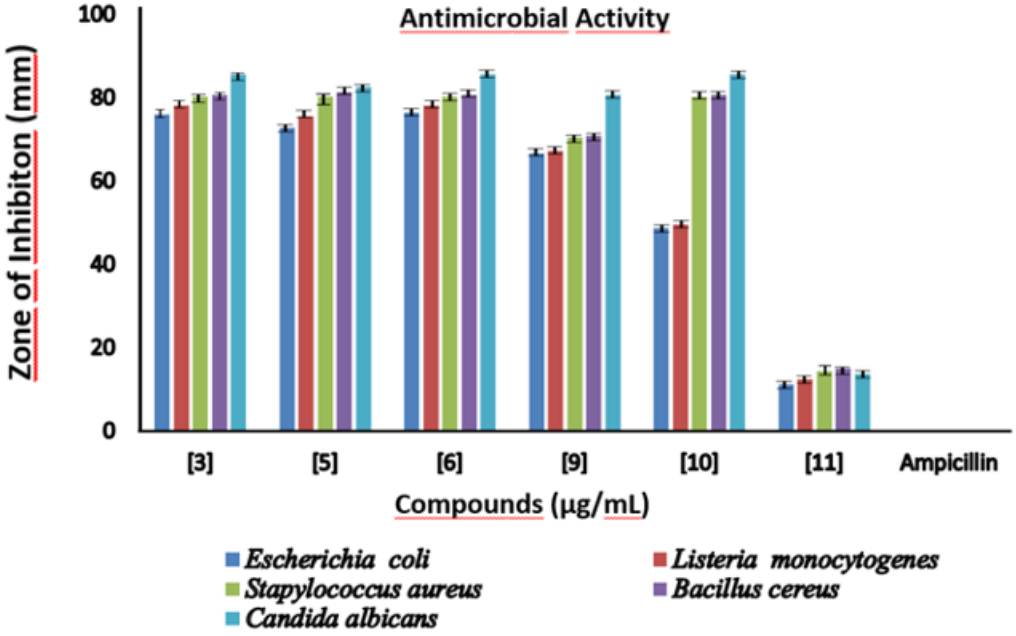

Figure. Antimicrobial measurements of synthesized compounds (The values given have the inhibition zone mean ± SE in millimeters).

Bacteria acquire resistance either by direct gene mutation or by obtaining the genes required for resistance from other bacteria. The synthesis of new compounds that can be used effectively in the treatment of infections and at the same time have as few side effects as possible constitutes one of the most important fields of study in chemistry today.

To combat the development of resistance, new antimicrobial compounds that have different structures and therefore are not recognized by microorganisms must be synthesized, or hybrid molecules containing several different pharmacophore groups in the same molecule must be obtained. All data show that the drugs currently used in the treatment of infections are either inadequate or ineffective for treatment, or the desired results cannot be achieved due to serious side effects. Therefore, it is important to synthesize new compounds and determine their antimicrobial activities.

The antimicrobial effects of the four ligands and their complexes obtained in this project were investigated at different concentrations against Gram-positive, Gram-negative and fungal strains. The high antimicrobial effect of the synthesized ligands and complexes, especially on Gram negative bacteria and fungi, gives hope for the future. It would be appropriate to test such substances on more bacterial species and at higher concentrations.

4. Conclusion

In this study, a new macrocyclic ligand containing Schiff base with many applications was synthesized; palladium complex of ligand numbered (**10**) was obtained during the

synthesis; the physical properties were defined after chemical structures, melting points, conductivities, and electrical measurements of all synthesized compounds were made by FTIR, ^{1}H-NMR, ^{13}C-NMR, LC-QTOF mass spectroscopy, thermogravimetric analysis (TGA-DTA) and ICP-MS methods. After this stage, antibacterial and antifungal properties were investigated. According to the results of our research, MIC values for the determined (**11**) complex were in the range of 11.25 µg/mL, which was higher than the 0.95 µg/mL potentials of positive controls such as ampicillin. The presented data show that Pd···Pd interactions, which were not supported in (**11**), were disrupted and dimeric Pd complexes (**10**) remained in this form in solution. As a result, the metallophilic interactions of these complexes are dissipated in solution. The distinct coordination environment of the binuclear complexes in solution (**11**), where Pd(II) is bound to the molecules, favored their stability. It has been shown that conformational fluidity in solution causes the [$C_{48}H_{38}Cl_2N_2O_2PdS_2$] complex to lose its copperophilic interactions. By utilizing the methods of obtaining the ligands obtained in this study, ligands with different chemical and physical properties can be synthesized and by binding different transition metals to these ligands, very promising results are obtained in terms of improving their antimicrobial activities.

Acknowledgments
This study received financial support from Trakya University Research Fund (TUBAP-2018-34)

Authors'Declaration
The authors declare no conflict of interests regarding the publication of this article.

AUTHOR CONTRIBUTIONS
All authors contributed to the writing of the manuscript by consensus.
Murat Türkyılmaz: concept, editing,
Murat Dönmez: analysis, writing, editing and submit; methodology.
All authors agree to be accountable of all aspects of the work.

References

1. M.N. Uddin, S.S. Ahmed, & S.R. Alam, Journal of Coordination Chemistry **73**(23) (2020) 3109.
2. A. Taha, N. Farooq, N. Singh, & A.A.Hashmi, Journal of Molecular Liquids **401** (2024) 124678.
3. E. Raczuk, B. Dmochowska, J. Samaszko-Fiertek, & J. Madaj, Molecules **27**(3) (2022) 787.
4. X. Chen, S. Zhang, Y. Jiang, G. He, M. Zhang, J. Wang, Z. Deng, H. Wang, J.W.Y. Lam, H. Lianrui, & B.Z. Tang, Angewandte Chemie **136**(19) (2024) e202402175.
5. J.N. Asegbeloyin, P.M. Ejikeme, L.O. Olasunkanmi, A.S. Adekunle, E.E. Ebenso, Materials **8**(6) (2015) 2918.
6. A. Mohammadzadeh, S. Javanbakht, R. Mohammadi, Colloids and Surfaces A: Physicochemical and Engineering Aspects **697** (2024) 134473.
7. R.J. Fessenden, S.S. Fessenden, Organic Chemistry, 4th. Ed. Brooks, Cole Publishing Company, California. (1980).
8. A.Z. El-Sonbati, W.H. Mahmoud, G.G. Mohamed, M.A. Diab, S.M. Morgan, S.Y. Abbas, Applied Organometallic Chemistry **33**(9) (2019) 5048.
9. A.T. Ali, A.I. Hamzah, A.H. Shather, A.J.H. Al-Athari, A.I. Oraibi, H.A. Almashhadani, Research on Chemical Intermediates **50** (2024) 1371.
10. N. Alhokbany, T. Ahamad, M. Naushad, S.M. Alshehri, Journal of Molecular Liquids **294** (2019) 111598.
11. Ö. Güngör, & L. Nuralin, Journal of Molecular Structure **1310** (2024) 138371.

12. Z. Wu, J. Xu, Z. Wu, R. Zhao, L. Hou, Journal of Photochemistry and Photobiology A: Chemistry **453** (2024) 115668.
13. R.M. Dhedan, S.A. Alsahib, R.A. Ali, Russian Journal of Bioorganic Chemistry **49**(1) (2023) S31.
14. M. Swathi, D. Ayodhya, Shivaraj, Results in Chemistry **7** (2024) 101231.
15. M. Aleshahidi, M. Gholizadeh, S.M. Seyedi, Research on Chemical Intermediates **48**(11) (2022) 4617.
16. L.H. Abdel-Rahman, M.T. Basha, B.S. Al-Farhan, W. Alharbi, M.R. Shehata, N.O.A. Zamil, D. Abou El-ezz, Molecules **28**(12) (2023) 4777.
17. R. Joshi, S. Pokharia, A. Singh, H. Mishra, K. Singh, Journal of Molecular Structure **1296** (2024) 136824.
18. A. Khalil, M.S.S. Adam, Molecules **29**(2) (2024) 414.
19. D. Sharma, H.D. Revanasiddappa, B. Jayalakshmi, Egyptian Journal of Basic and Applied Sciences **7**(1) (2020) 323.
20. B. Kumar, J. Devi, A. Dubey, A. Tufail, & S. Sharma, Inorganic Chemistry Communications **159** (2024) 111674.
21. A. Bhardwaj, M. Kumar, A. Bendi, & S. Garg, Chemistry & Biodiversity **21**(2) (2024) 202301544.
22. C. Fei, W. Gao, J. Zhang, Z. Wu, Y. Lv, & H. Wu, Journal of Molecular Structure **1308** (2024) 138069.
23. A. Toghan, O.K. Alduaij, A. Fawzy, A.M. Mostafa, A.M. Eldesoky, A.A. Farag, ACS Omega **9**(6) (2024) 6761.
24. S. Thakur, & A. Bhalla, Tetrahedron **153** (2024) 133836.
25. Z. Zhang, Q. Song, Y. Jin, Y. Feng, J. Li, & K. Zhang, Metals **13**(2) (2023) 386.
26. M. Abdallh, M. Bufaroosha, A. Ahmed, D.S. Ahmed, & E. Yousif, Journal of Vinyl and Additive Technology **26**(4) (2020) 475.
27. E. Keskioğlu, A.B. Gündüzalp, S. Cete, F. Hamurcu, B. Erk, Spectrochimica Acta Part A: Molecular and Biomolecular Spectroscopy **70**(3) (2008) 634.
28. O. Hakami, A.N.M. Alaghaz, T. Zelai, & S.A. Albohy, Applied Organometallic Chemistry **38**(6) (2024) 7488.
29. L. Man, H. Chen, H. Deng,H. Zhou, L. Hao, & X. Zhou, Applied Clay Science **256** (2024) 107429.
30. R. Nirmal, K. Meenakshi, P. Shanmugapandiyan, C.R. Prakash, Journal of Young Pharmacists **2**(2) (2010) 162.
31. I. Kostova, Inorganics **11**(2) (2023) 56.
32. X.H. Ding, L.Z. Wang, Y.Z. Chang, C.X. Wei, J.Y. Lin, M.H. Ding, & W. Huang, Aggregate **5**(3) (2024) 500.
33. B.K. Seth, A. Ray, M. Banerjee, T. Bhattacharyya, D. Bhattacharyya, S. Basu, Journal of Luminescence **171** (2016) 85.
34. S. Jhaumeer-Laulloo, M.G. Bhowon, S. Mungur, M.F. Mahomoodally, & A.H. Subratty, Medicinal Chemistry **8**(3) (2012) 409.
35. B.A. Benedict, International Journal of Chemistry **4**(1) (2015) 22.
36. B. Dag, Y. Tenekecioğlu, T. Aral, H. Kızılkaya, R. Erenler, N. Genc, Russian Journal of Bioorganic Chemistry **49** (2023) 861.
37. S. Bozkurt, Master Thesis Selçuk University, Konya (2022).
38. H. Keypour, R. Azadbakht, & H. Khavasi, Polyhedron **27**(2) (2008) 648.
39. R.M. Ahmed, E.I. Yousif, H.A. Hasan, & M.J. Al-Jeboori, The Scientific World Journal **2013**(1) (2013) 289805.
40. W. Radecka-Paryzek, V. Patroniak, & J. Lisowski, Coordination Chemistry Reviews **249**(21-22) (2005) 2156.
41. A.E.F. Ouf, M.S. Ali, E.M. Saad, S.I. Mostafa, Journal of Molecular Structure **973**(1-3) (2010) 69.

42. M.M. Omar, H.F.A. El-Halim, E.A. Khalil, Applied Organometalic Chemistry **31** (2017) 3724.
43. A. Xavier, N. Srividhya, IOSR Journal of Applied Chemistry **7**(11) (2014) 6.
44. E. Jaziri, H. Louis, C. Gharbi, T.O. Unimuke, E.C. Agwamba, G.E. Mathias, W. Fugita, C.B. Nasr, L. Khedhiri, Journal of Molecular Structure **1268** (2022) 133733.
45. W. Radecka-Paryzek, V. Patroniak, & J. Lisowski, Coordination Chemistry Reviews **249**(21-22) (2005) 2156.
46. R.M. Ahmed, E.I. Yousif, H.A. Hasan, M.J. Al-Jeboori, The Scientific World Journal **2013**(1) (2013) 289805.
47. T.A. Alorini, A.N. Al-Hakimi, S.E.-S. Saeed, E.H.L. Alhamzi, A.E. Albadri, Arabian Journal of Chemistry 15 (**2022**) 103559.
48. J.N. Asegbeloyin, P.M. Ejikeme, L.O. Olasunkanmi, A.S. Adekunle, E.E. Ebenso, Materials **8**(6) (2015) 2918.
49. M.S. Al-Fakeh, N.F. Al-Otaibi, Journal Nanotechnology **2022** (2022) 7794939.
50. E.G. Karimli, V.N. Khrustalev, M.N. Kurasova, M. Akkurt, A.N. Khalilov, A. Bhattarai, I.G. Mamedov, Acta Crystallographica Section E **79**(5) (2023) 474.
51. F.N. Naghiyev, T.A. Tereshina, V.N. Khrustalev, M. Akkurt, A.N. Khalilov, A.A. Akobirshoeva, I.G. Mamedov, Acta Crystallographica Section E **77**(5) (2021) 512.
52. A.N. Khalilov, J. Cisterna, A. Cárdenas, B. Tuzun, S. Erkan, A. V. Gurbanov, I. Brito. Synthesis, Journal of Molecular Structure **1313** (2024) 138652.
53. V.G. Nenajdenko, A.A. Kazakova, A.S. Novikov, N.G. Shikhaliyev, A.M. Maharramov, A.M. Qajar, G.T. Atakishiyeva, A.A. Niyazova, V.N. Khrustalev, A.V. Shastin, A.G. Tskhovrebov, Catalysts **13**(8) (2023) 1194.
54. A. Maharramov, N.Q. Shikhaliyev, A. Abdullayeva, G.T. Atakishiyeva, A. Niyazova, V.N. Khrustalev, S.I. Gahramanova, Z. Atioğlu, M. Akkurt, A. Bhattarai, Acta Crystallographica Section E **79**(10) (2023) 905.
55. A. Maharramov, N.Q. Shikhaliyev, A. Qajar, G.T. Atakishiyeva, A. Niyazova, V.N. Khrustalev, M. Akkurt, S.Ö. Yıldırım, A. Bhattarai, Acta Crystallographica Section E **79**(7) (2023) 637.
56. M.S. Al-Fakeh, G.A. Allazzam, N.H. Yarkandi, Sylwan **165**(9) (2021) 198.
57. M.S. Al-Fakeh, G.A. Allazzam, N.H. Yarkandi, International Journal Biomaterials **2021** (2021) 4981367-1.
58. M.S. Al-Fakeh, S. Messaoudi, F.I. Alresheedi, A.E. Albadri, W.A. El-Sayed, E.E. Saleh, Crystals **13**(1) (2023) 118.
59. M.S. Al-Fakeh, Biochemistry and Biotechnology Research **5**(2) (2017) 30.
60. C.E. Satheesh, P.R. Kumar, P. Sharma, K. Lingaraju, B.S. Palakshamurthy, & H.R. Naika, Inorganica Chimica Acta **442** (2016)
61. H.C. Ansel, W.P. Norred, & I.L. Roth, Journal Of Pharmaceutical Sciences **58**(7) (1969) 836-839.
62. K.D. Loncar, R.A. Ferris, P.M. McCue, G.I. Borlee, M.L. Hennet, & B.R. Borlee, Journal of Equine Veterinary Science **53** (2017) 94.
63. A. Mohammadzadeh, S. Javanbakht, & R. Mohammadi, Colloids and Surfaces A: Physicochemical and Engineering Aspects **697** (2024) 134473.
64. M. Ghosh, S. Mandal, M. Fleck, R. Saha, C. Rizzoli, & D. Bandyopadhyay, Journal of Coordination Chemistry **71**(24) (2018) 4180.